

BCSJ Award Article

Preparation and Characterization of Spherical and Balloon-Like Calcium Phosphate Particles

Kazuhiko Kandori,*[1] Kiri Tada,[1] Masao Fukusumi,[2] and Yoshiaki Morisada[2]

[1]School of Chemistry, Osaka University of Education, 4-698-1 Asahigaoka, Kashiwara, Osaka 582-8582

[2]Department of Processing Technology, Osaka Municipal Technical Research Institute, 1-6-50 Morinomiya, Joto-ku, Osaka 536-8553

Received June 20, 2008; E-mail: kandori@cc.osaka-kyoiku.ac.jp

Calcium phosphate particles were prepared by aging a solution of $CaCl_2$ and sodium triphosphate (sodium tripolyphosphate, Natpp: $Na_5P_3O_{10}$) at 100–150 °C for 16 h in a Teflon-lined screw-capped Pyrex test tube. The rod-like and spherical particles were precipitated at an extremely fast rate of reaction under 100 °C. The spherical particles were only produced in a very narrow region at 100 °C by aggregation of primary small particles. The rod-like particles were $CaNa_2P_2O_7 \cdot 4H_2O$ but the uniform spherical ones were amorphous and the latter ones were crystallized to β-$Ca_2P_2O_7$ after being calcined above 600 °C. The aging temperature drastically varied the particle shape under conditions for producing uniform spherical particles; solid spherical particles were produced up to the aging temperature of 115 °C but balloon-like hollow spheres were precipitated at 120 °C. However, large and irregular agglomerates made up of extremely small rod-like particles were precipitated after aging the solution above 125 °C. TEM observation and ICP-AES measurements revealed that the balloon-like hollow spheres were produced by dissolving the interior of solid spherical particles after reinforced their shell by the adsorption of unhydrolyzed tpp. The spherical and balloon-like calcium phosphate particles with amorphous crystal form showed high selective adsorption of H_2O by rehydration of Ca^{2+} ions by penetrated H_2O molecules into the particles. In particular, the balloon-like hollow spheres of calcium phosphate may hold potential as drug delivery vehicles and have biocompatibility advantages.

Various metal phosphates have many applications in pigments, catalysis, adsorbents, and bioceramics.[1,2] In order to develop the materials into high-quality products, studies on the preparation and characterization of uniform spherical metal phosphate particles have been extensive.[3–7] In the last decade, Kandori et al. have investigated the inner structure of these uniform particles and found that cobalt phosphate particles possess a thermally unstable layer structure which exhibits a high selective adsorption of H_2O by molecular sieve effects,[8] while nickel,[9] aluminum,[10–12] and ferric phosphate[13] particles are agglomerates of fine primary particles which exhibit high mesoporosity. In the case of aluminum phosphate particles, we succeeded in controlling the particle size by using urea and isopropylamine[11] and metal ions.[12] On the other hand, the authors have investigated calcium hydroxyapatite ($Ca_{10}(PO_4)_6(OH)_2$, HAp) as an adsorbent material for liquid chromatography, because HAp is a major inorganic component of biological hard tissues.[14–17] Although HAp is a metal phosphate, controlling the particle shape and size is very difficult because of its low solubility product. Since the hydrolysis of condensed phosphate ions, such as diphosphate (pyrophosphate, pp: $P_2O_7^{4-}$) and triphosphate (tripolyphosphate. tpp: $P_3O_{10}^{5-}$) ions, is an endothermic process,[18–20] the phosphate (orthophosphate: PO_4^{3-}) ions can be produced slowly by heating the solution, a so called forced hydrolysis reaction. Therefore, it can be expected that the forced hydrolysis reaction of the mixed solution of Ca^{2+} and condensed phosphate ions can be applied for producing new calcium phosphate particles with unique shape and inner structure. Thus, this study was conducted as a continuation of previous studies to investigate control of the size and structure of calcium phosphate particles. The results of this study will yield insight into the formation, structure, and adsorption properties of the spherical and/or balloon-like calcium phosphate particles. The formation mechanism of fairly uniform and transparent balloon-like hollow spheres is also proposed.

Experimental

Materials. Following the method reported by the authors for producing ferric phosphate particles,[13] we produced calcium phosphate particles by aging a solution of $CaCl_2$ (1.0×10^{-3}–1.0×10^{-1} mol dm^{-3}) and Natpp (1.0×10^{-3}–1.0×10^{-1} mol dm^{-3}) in a 20-cm^3 Teflon-lined screw-capped Pyrex test tube. In this study, sodium triphosphate (Natpp: $Na_5P_3O_{10}$) was used instead of H_3PO_4. To facilitate the aging, the test tubes were allowed to stand for 16 h at various temperatures (100–150 °C) in

Published on the web December 12, 2008; doi:10.1246/bcsj.81.1567

a convection oven. The resulting particles were thoroughly washed by filtration with deionized and distilled water and finally dried in an air-oven at 70 °C for 16 h. The solution pH before and after aging was monitored at room temperature. Guaranteed reagent grade chemicals from Wako Pure Chemical Co., Inc. were used without further purification.

Characterization. The resulting particles were characterized by transmission electron microscope (TEM), thermogravimetry and differential thermal analysis (TG-DTA), Fourier transform infrared spectrophotometery embedded in KBr pellets (0.2 wt %) (FTIR), powder X-ray diffraction measurement (XRD), adsorption experiments of N_2 and H_2O as those employed in our previous work.[8–13] The adsorption isotherms of N_2 were measured at liquid N_2 temperature with an ordinary house built automatic volumetric flow method using a Baratron diaphragm manometer attached to a mass flow meter. On the other hand, those of H_2O were measured at 25 °C with a computer aided automatic gravimetric method using a quartz spring balance. The degrees of confidence on specific surface areas measured by these apparatuses were within 2%. Prior to these gas adsorption measurements, the samples were evacuated at 25 °C for 2 h. The chemical composition of the precipitated particles (concentration of calcium and phosphorus) was determined by dissolving a few milligrams in concentrated nitric acid. The solutions were diluted and the calcium and phosphorus concentrations were determined by inductively coupled plasma atomic emission spectroscopy (ICP-AES).

Results and Discussion

Particle Morphology and Crystal Form. Figure 1 displays (a) the solution pH and (b) morphology and crystal form of the particles precipitated after aging the solution for 16 h at 100 °C. The gray circles suggest the solution produced precipitates before aging. Thus no forced hydrolysis reaction was employed for these systems. The solution pH of 8.61–9.82 dropped 1.5–2.0 units after reaction. It has been reported that the hydrolysis of tpp ions is expressed as the following two reactions (1) and (2).[21]

$$P_3O_{10}^{5-} + 2H_2O \rightarrow 3PO_4^{3-} + 4H^+ \quad (1)$$

$$2P_3O_{10}^{5-} + H_2O \rightarrow 3P_2O_7^{4-} + 2H^+ \quad (2)$$

The reaction (1) represents that tpp ions are completely hydrolyzed to orthophosphate ions. In the case of the reaction (2), tpp ions are not completely hydrolyzed and still remain pp ions. Since the solutions are almost neutral after the reaction (pH 7.02–7.75), the protonated states of orthophosphate (HPO_4^{2-}) and pyrophosphate ($HP_2O_7^{2-}$) ions were ignored in the reactions (1) and (2). Both the reactions generate protons in any event. Therefore, the pH drop watched in this experiment proves that the tpp ions were hydrolyzed. Figure 2 shows the TEM pictures of typical particles precipitates at A, B, C, and D points in Figure 1 together with their Ca/P molar ratios. Clearly, calcium pyrophosphates ($Ca_2P_2O_7 \cdot 4H_2O$; JSPDS 00-009-0346 and α-$CaNa_2P_2O_7 \cdot 4H_2O$; JCPDS 97-002-0572) with a rod-like shape are produced at higher concentration of tpp ions. On the other hand, amorphous and spherical particles are produced at other concentration domains. It should be emphasized that the monodispersity of spherical particles (sample C) is high. The preparation conditions of calcium phosphate particles characterized in the following sections are listed in Table 1.

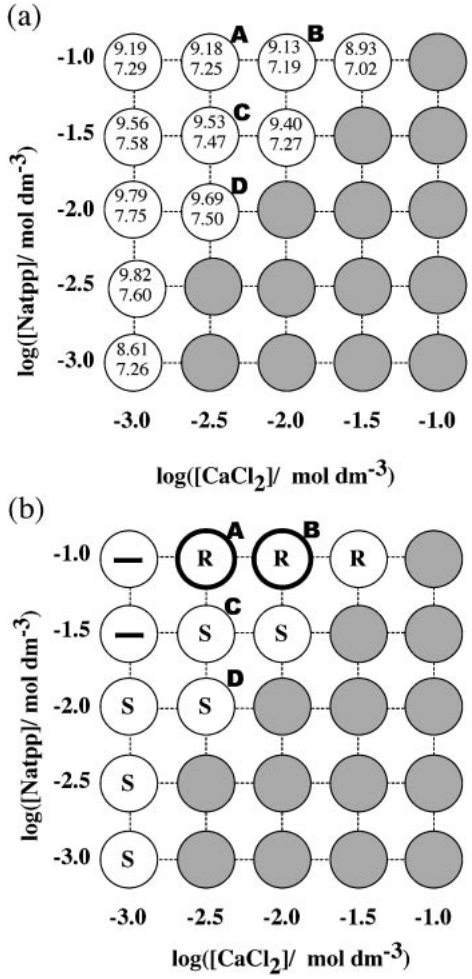

Figure 1. (a) The pH and states of mixed solutions of $CaCl_2$ and Natpp for aging at 100 °C. Upper and lower numbers are solution pH before and after aging, respectively. Gray circles indicate the solution produced precipitates before aging. (b) Particle shape and crystalline form of precipitates after aging. R: rod-like, S: spheres. Thin and thick circles of samples A and B indicate amorphous, $Ca_2P_2O_7 \cdot 4H_2O$ and α-$CaNa_2P_2O_7 \cdot 4H_2O$, respectively. A bar in the circle indicates no precipitate after aging.

The XRD patterns of samples A and C after being calcined at various temperatures in air for 2 h are displayed in Figure 3. Crystallization was observed on sample A after heating at 600 °C for 2 h in air although it was amorphous at 200–400 °C. The amorphous sample C crystallized to β-$Ca_2P_2O_7$ after heating at 600 °C for 2 h. Both samples A and C contain pp ions, suggesting that the hydrolysis reaction of tpp ions was incomplete as is the following reaction (1). The Ca/P molar ratio of the sample A is 0.66, suggesting that the composition of sample A can be described as α-$CaNa_2(P_2O_7)_{0.76}(OH)_{0.96} \cdot 4H_2O$ by assuming that a portion of $P_2O_7^{4-}$ ions are exchanged to OH^- ions. The Ca/P molar ratio of sample B is 0.99, coinciding with the unity of its crystal form. The Ca/P molar ratios of spherical and amorphous C and D particles are widely varied, depending on the samples. The spherical particles produced in the present study are analogous to $Ni_3(PO_4)_2$, $AlPO_4$, and $FePO_4$ as the authors re-

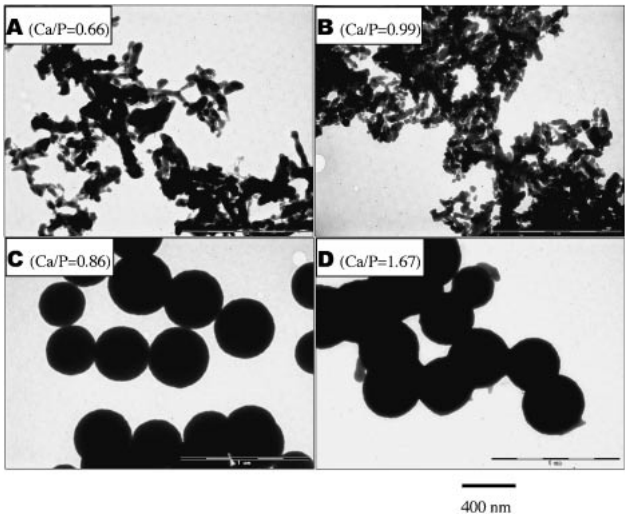

Figure 2. TEM pictures of typical samples A, B, C, and D in Figure 1.

Table 1. Preparation Conditions of Calcium Phosphate Particles Characterized

Sample	log([$CaCl_2$] /mol dm^{-3})	log([Natpp] /mol dm^{-3})	Aging temperature/°C
A	−2.5	−1.0	100
B	−2.0	−1.0	100
C (C-100)	−2.5	−1.5	100
D	−2.5	−2.0	100
C-110	−2.5	−1.5	110
C-115	−2.5	−1.5	115
C-120	−2.5	−1.5	120
C-125	−2.5	−1.5	125
C-130	−2.5	−1.5	130
C-140	−2.5	−1.5	140
C-150	−2.5	−1.5	150

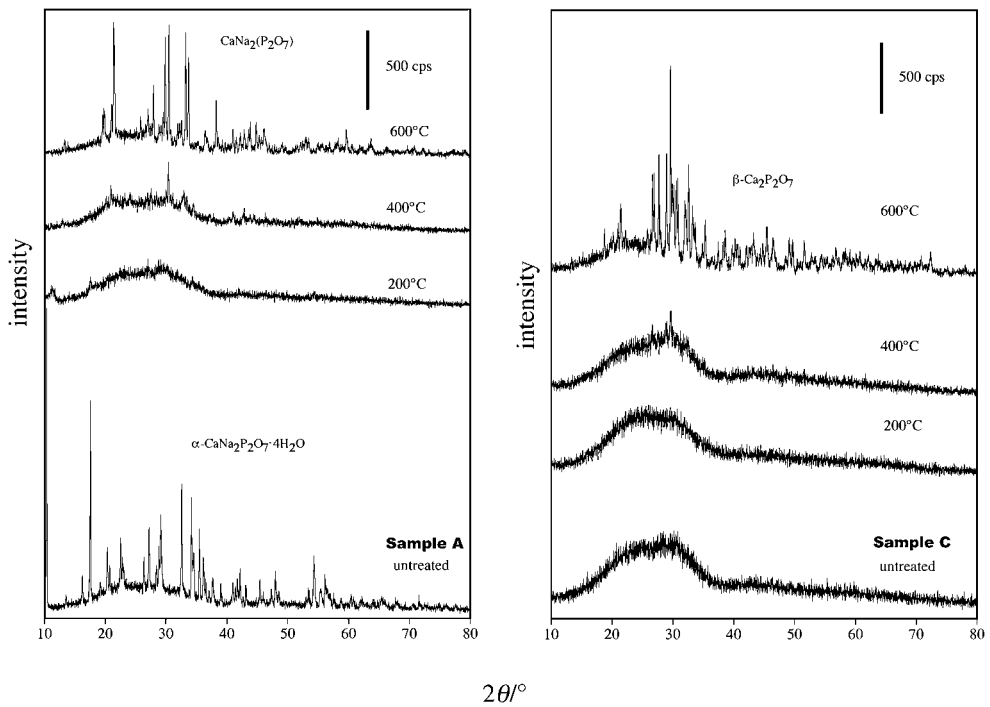

Figure 3. XRD patterns of samples A and C in Figure 1.

ported in our previous papers.[9–13] It has been established by Morales et al. that solid metal phosphates adsorb protons, which is responsible for their catalytic activity.[22] They revealed that the proton adsorption at the beginning of nucleation completely blocks the supercritical nuclei, thus preventing their development to visible primary particles. A similar mechanism can be adapted to the present study. In the first step, nucleation occurs at an outburst speed forming a large number of primary particles. Probably, this reaction is faster than adsorption of tpp ions. Actually, the precipitates abruptly appeared after aging 2 h in the present study. Hence, these primary particles aggregate in a spherical morphology because this gives the minimum total surface free energy for a given volume. In the second step, unhydrolyzed tpp molecules are adsorbed onto the spherical particles. In practice, the aggregated structure was observed by TEM observation though the data is not shown.

The crystallization of sample C to β-$Ca_2P_2O_7$ was further confirmed by TG-DTA measurement as is shown in Figure 4. The small exothermic peak can be recognized at 520 °C in the DTA curves on sample C. In addition, a large endothermic peak appears at ca. 25–160 °C together with a large weight loss (ca. 10 wt %) in the TG curves. This endothermic peak and weight loss are due to loss of water molecules remaining in poorly ordered amorphous particles. For sample A, one more endothermic peak and TG weight loss appear ca. 150–200

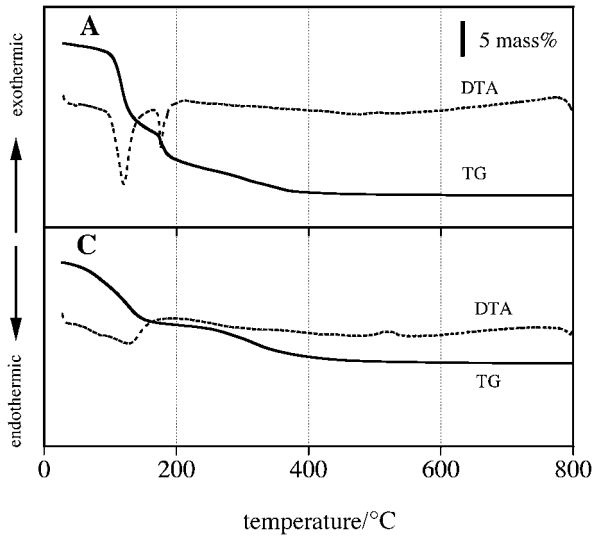

Figure 4. TG-DTA curves of samples A and C in Figure 1.

°C. This peak can be naturally identified as an elimination of water of crystallization.

Effects of Forced Hydrolysis Temperature. In the previous section, it was clear that the aging temperature of 100 °C is insufficient to completely hydrolyze tpp ions; in other words, the preparation of HAp and other calcium orthophosphate particles is difficult at 100 °C. In order to increase the degree of hydrolysis of tpp ions, the aging temperature was varied from 100 to 150 °C (samples C-100 to C-150) under the condition for producing monodisperse spherical particles (sample C: see in Table 1). Figure 5 shows the TEM pictures of sample C formed at various aging temperatures together with their Ca/P molar ratios. Clearly, the spherical particles are produced up to 110 °C. However, hollow spheres can be seen at 115 °C and finally transparent balloon-like hollow spheres can be recognized at 120 °C. The wall thickness of the balloon-like hollow spheres is approximately 10–20 nm (measured from TEM micrographs). The large spherical particles are produced together with balloon-like ones at 125 °C. At above 130 °C, no balloon-like hollow spheres are recognized but small rod-like particles are detected. The XRD patterns of those particles are shown in Figure 6. The spherical particles and/or balloon-like hollow spheres are amorphous, but the characteristic peaks of HAp (JCPDS 9-432) appear for the samples produced above 130 °C though their crystallinity is low with small S/N ratio. The Ca/P molar ratios of amorphous particles are 0.82–0.96 though those values increased to 1.38–1.48 by raising the aging temperature. Even though the XRD patterns suggest HAp crystal form, the Ca/P molar ratios of these particles are less than the stoichiometric value of 1.67. This fact indicates that the HAp particles are Ca-deficient with low crystallinity.

The FTIR spectra of these particles are shown in Figure 7. The amorphous particles produced at 100–125 °C have peaks at 925, 1055, and 1135 cm^{-1} due to stretching vibration bands of phosphate groups in amorphous calcium phosphate crystal together with an absorption band at 562 cm^{-1}: from a bending mode of O–P–O. On the other hand, the HAp particles produced above 130 °C exhibit a large band at 1000–1100 cm^{-1} with a peak at 1040 cm^{-1} due to the stretching vibration of orthophosphate groups and those at 569 and 604 cm^{-1} by a bending mode of orthophosphate groups. These data coincide well with the results of XRD.

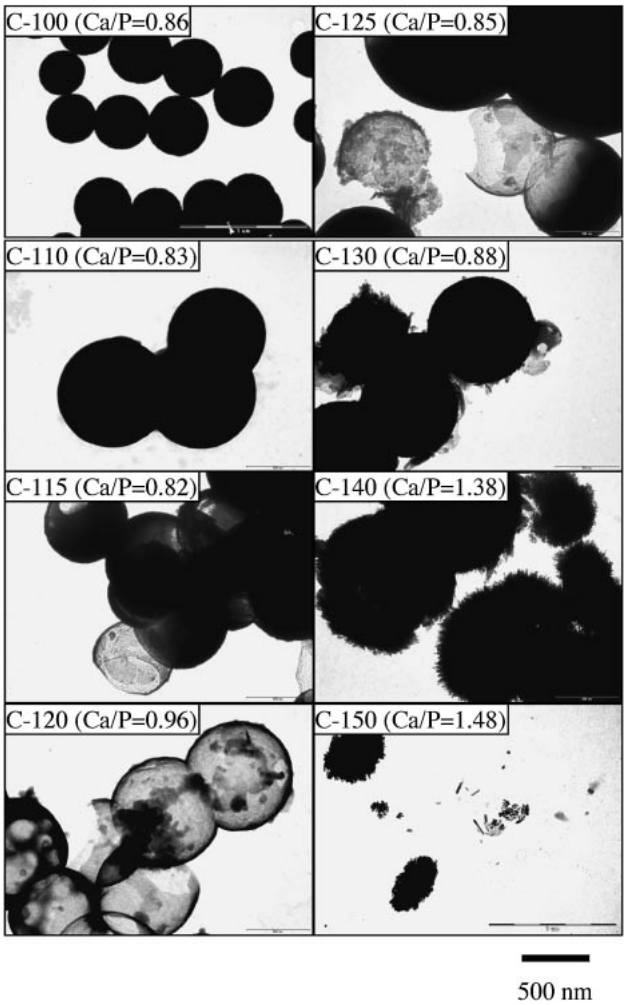

Figure 5. TEM pictures of C-100, -110, -115, -120, -125, -130, -140, and -150 particles.

In Figure 5, we successfully prepared the calcium phosphate particles with fairly uniform and transparent balloon-like structure. Hollow spheres with nano to micrometer dimensions have attracted great investigative interests because of their various application potentials, such as in catalysts, dyes or inks, coatings, fillers, and microreactors. Various efforts have been made to prepare inorganic hollow spheres by using different templates, including polyelectrolyte nano-particles,[23] emulsion droplet,[24,25] polymer micelles,[26] or simply a sacrificial metastable precursor phase.[27] Recently, double hydrophilic block copolymer (DHBC) and mixed solvents of surfactants and DHBC have also been used as templates for preparing $CaCO_3$ hollow spheres by Cölfen.[28] They explained that the hollow spheres develop from spheres by a dissolution process staring at the center of the sphere. Qi et al. reported the synthesis of micrometer sized calcite hollow spheres by the cooperative effect of DHBC–surfactant complex micelles as the templates.[29] Furthermore, many methods already reported for the synthesis of calcium phosphate particles including microemulsion tem-

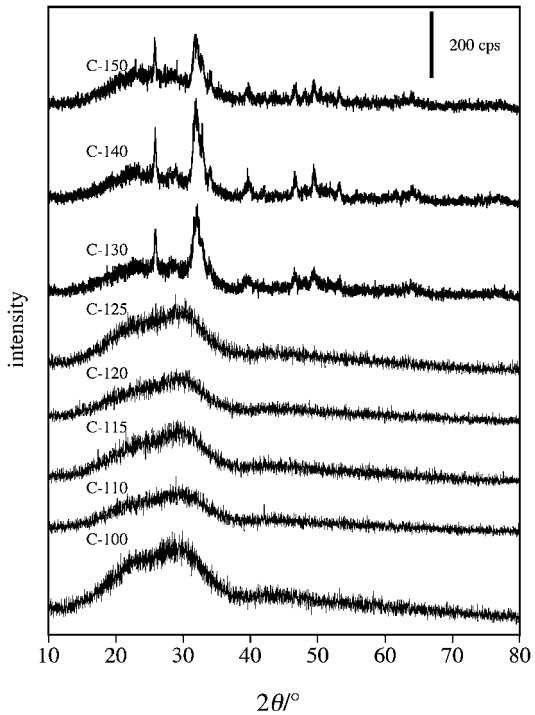

Figure 6. XRD patterns of particles as is shown in Figure 5.

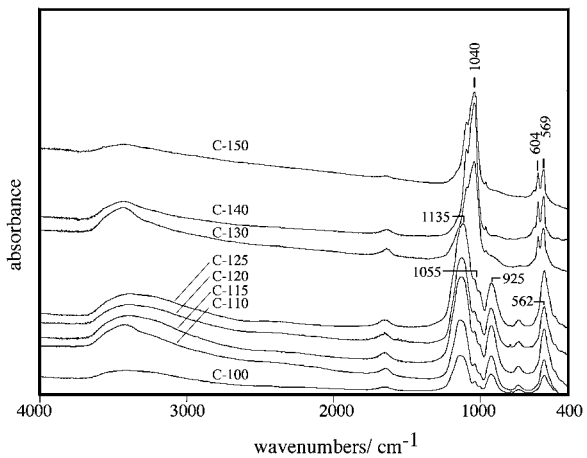

Figure 7. FTIR spectra of particles as is shown in Figure 5.

plating,[30] ultrasonic spray pyrolysis,[31] emulsion templating,[32] block copolymer templating,[33] polyelectrolyte-mediated crystallization,[34] and high-temperature ceramic methods.[35] However, the size of hollow particles reported in these papers were large and they possess unequal surfaces with porous shells. Even though they produce nanoparticles,[32,33] the preparation methods include complicated procedures such as calcinations for removing the templates. Comparing to these particles, the present work is a simple single pot method and balloon-like hollow spheres produced in this experiment have unique structures, i.e., fairly uniform, transparent and smooth surface. Therefore, it is worthwhile to elucidate the formation mechanism of this unique structure. Thus, a detailed time-dependent experiment was conducted at 120 °C to track the formation of balloon-like particles in the next section.

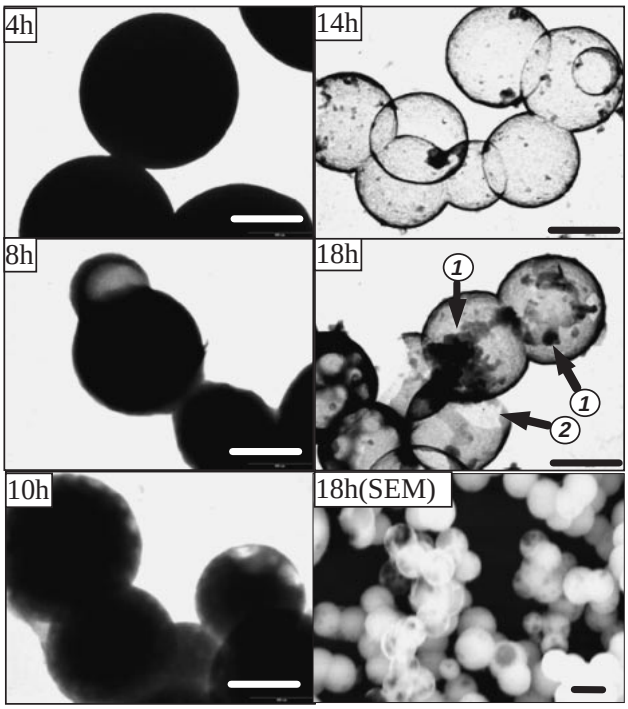

Figure 8. Time-resolved TEM and SEM (18 h) pictures of precipitates for producing balloon-like particles at 120 °C (C-120) in Figure 5. Scale bars in the pictures represent 500 nm.

Figure 8 illustrates time-resolved TEM pictures of precipitates for producing the balloon-like particles at 120 °C in Figure 5. When the hydrolysis reaction was conducted for 4 h, many solid spherical particles ca. 500–1000 nm in diameter are produced. The reaction was further continued for 8 h, some spherical particles with pale centers began to form. Upon further prolonging of the reaction time to 10 h, the inside of the hollow particles becomes pale and finally transparent balloon-like hollow spheres are formed after aging for 14 h. The SEM pictures of the balloon-like hollow spheres are also shown in Figure 8. These TEM and SEM results suggest that the balloon-like hollow spheres were formed by dissolution of the interior of solid spherical particles.

To confirm this assumption, the concentrations of phosphate ([P]) and calcium ([Ca]) ions were measured by ICP. The results are displayed in Figure 9. Clearly, the [Ca] values decrease steeply for 10 h, but [P] values reduce only 20%, suggesting that an aging temperature of 120 °C is still insufficient to hydrolyze completely tpp ions. Another finding in Figure 9 is both the [Ca] and [P] values reach a maximum at 12 h. These increases of [Ca] and [P] strongly support that the inside of the solid spherical particles has dissolved. However, these values decreases quickly again on further aging. This decrease is probably due to the production of small calcium phosphate particles as can be seen in TEM pictures produced after 18 h in Figure 8 (shown by arrows 1). In addition, from the TEM micrograph of the balloon-like hollow spheres, many of the spheres appear to be fused together as a consequence of this dissolution–reprecipitation process. A similar effect of adsorbed polymeric materials for producing hollow spheres has been reported.[36] Uniform CuS hollow spheres of ca. 40 nm were

produced by oxidation of S^{2-} in CuS particles with air using a Cu^{2+}–trimethylenediamine chelate system in the presence of ammonia and gelatin. In this system, adsorbed gelatin inhibits the oxidation of the external sulfide in the surface layer of CuS particles while allowing the diffusion of oxygen into the interiors.

Since tpp ions have very strong adsorption ability to the HAp surface as the authors have already revealed,[37] the unhydrolyzed tpp ions (ca. 80%) would be adsorbed on the solid spherical particles initially produced. The adsorption of tpp ions may protect the dissolution of particle shells resulting in the balloon-like structure. Of course, it can be anticipated that the places where tpp ions weakly adsorbed can become an evolution point for particle dissolution. Indeed, some balloon-like particles burst and the cleft structure can be seen in the TEM picture (shown by arrow 2). The explanation of this formation mechanism will be the subject of further work. Hollow spheres of calcium phosphate hold potential as drug delivery vehicles, for example, and have biocompatibility advantages over other materials.

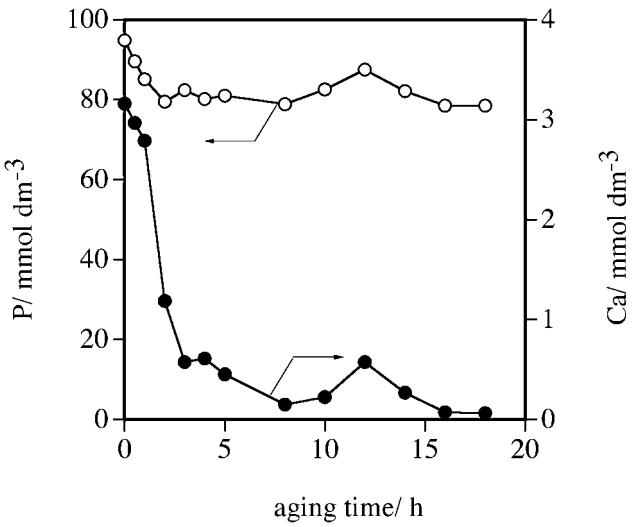

Figure 9. Changes of concentrations of phosphate and calcium ions in the aging solution for producing balloon-like particles at 120 °C (C-120).

Adsorptive Properties. We found in previous work that the $AlPO_4$[11] and $Ni_3(PO_4)_2$[9] particles exhibit a high selective adsorption of H_2O though they adsorb small amounts of N_2. Since the calcium phosphate particles prepared in this work contain a large amount of hydrated H_2O molecules as discussed before, it can be expected that similar characteristic adsorptive properties will emerge. To reveal this point, we measured N_2 and H_2O adsorption isotherms for the samples prepared at varied aging temperature as shown in Figure 5.

All the N_2 adsorption isotherms for the particles outgassed at 25 °C were of Type II in the BDDT classification[38] as shown in Figure 10a. Clearly, the amounts of adsorbed N_2 increase with increasing aging temperature for particle preparation for the samples C-110 to C-140, though they slightly decrease for C-150. However, they did not change significantly by changing the evacuation temperature from 25 to 300 °C in each sample (data not shown). The specific surface area (S_n) of the samples was calculated by applying the BET equation to these N_2 adsorption isotherms using a cross-sectional area of N_2 molecule of 0.162 nm^2. The measured S_n values after evacuated at 25 °C are plotted in Figure 11 by open circles as a function of aging temperature. The S_n values remain almost constant at ca. 3–5 $m^2\,g^{-1}$ up to an aging temperature of 125 °C, though they increase steeply up to 80 $m^2\,g^{-1}$ at 130 °C. The specific surface area of 80 $m^2\,g^{-1}$ corresponds to a particle diameter of 25 nm by assuming a density of 3 g cm^{-3} using the following equation, $S = 6/D\rho$, where S, D, and ρ are specific surface area, diameter, and density of the solid spheres, respectively. The evaluated particle diameter is in fair agreement with the size of small rod-like HAp particles. All H_2O adsorption isotherms for these particles were also Type II in the BDDT classification as well as N_2 adsorption as shown in Figure 10b. The amounts of adsorbed H_2O decreased with increased aging temperature for particle preparation from C-100 to C-125, while they increase again from C-130 to C-150 due to the reduction of particle size. The specific surface area (S_w) of the samples was calculated by using a cross-sectional area of an H_2O molecule (0.108 nm^2). To compare the adsorption selectivity of H_2O, the S_w/S_n ratio was calculated and plotted as a function of aging temperature in Figure 11 (solid circles). The large S_w/S_n ratio (38) is observed for the particles produced at 100 °C (C-100)

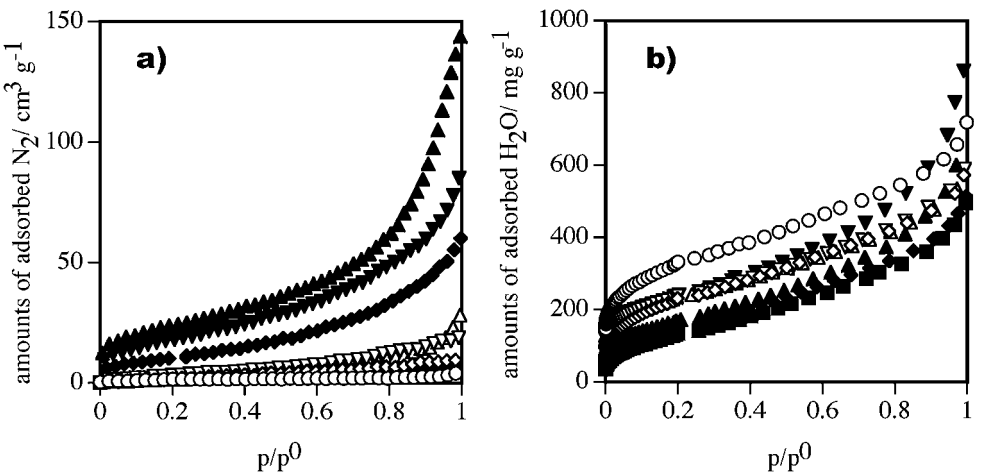

Figure 10. Adsorption isotherms of (a) N_2 and (b) H_2O molecules onto the C-100 (○), -110 (◇), -115 (▽), -120 (△), -130 (◆), -140 (▲), and -150 (▼) particles after evacuated at 25 °C.

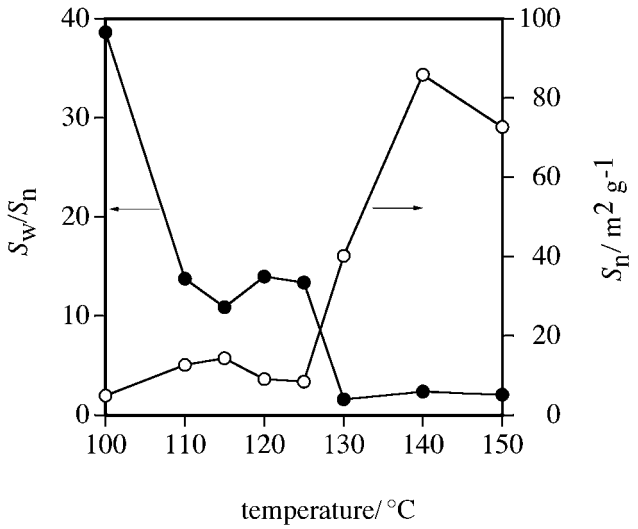

Figure 11. Plots of specific surface area measured by using N_2 (S_n) and selectivity of H_2O adsorption (S_w/S_n) as a function of aging temperature under conditions for producing balloon-like particles.

and they decrease slightly to 10–15 after elevating the aging temperature up to 110–125 °C, indicating that high selective adsorption of H_2O is achieved for those amorphous particles. However, they decrease to ca. 2 above 130 °C. Similar high adsorption selectivity of H_2O was observed on amorphous $AlPO_4$ particles,[11,12] which can be explained by rehydration of the particles by adsorbed H_2O. A similar fact was reported in the case of chromium gel prepared from chromium nitrate solution utilizing the slow hydrolysis of urea.[39] The hydrogels, freshly formed from highly hydrated Ca^{2+} ions in the present study, are usually poorly ordered and retain considerable amounts of hydrated H_2O. These hydrated H_2O molecules are removed by outgassing without an appreciable structural change or collapse of the solid framework. The cavities formed near the cations by outgassing serve for H_2O adsorption but not for N_2. Thus, the rehydration of Ca^{2+} ions by H_2O penetrated in the cavities may take place due to the coordination of adsorbed H_2O to Ca^{2+} ions. Indeed, the adsorption selectivity of H_2O reduced by crystallization of particles after elevating the evacuation temperature above 200 °C. This high selective adsorption of H_2O suggests that the amorphous calcium phosphate particles can be applied as adsorbent.

Conclusion

1) The preparation procedure employed in this work precipitated rod-like, spherical, and balloon-like calcium phosphate particles. The solid spherical particles were only produced in a very narrow region.

2) The amorphous particles grew in spherical structure by aggregation of primary small particles.

3) The rod-like and spherical particles crystallized to $CaNa_2P_2O_7$ and β-$Ca_2P_2O_7$, respectively, after the particles were calcined above 600 °C in air.

4) The balloon-like hollow spheres were produced only by aging at 120 °C and they were formed by dissolving the interior of solid spherical particles after reinforced their shell by the adsorption of tpp ions.

5) The spherical and amorphous calcium phosphate particles exhibited a high selective adsorption of H_2O by rehydration into the amorphous particles.

References

1 E. Susa, *J. Polym. Sci., Part C: Polym. Symp.* **1963**, *4*, 399.
2 C. P. A. T. Klein, A. A. Driessen, K. de Groot, A. van den Hoff, *J. Biomed. Mater. Res.* **1983**, *17*, 769.
3 E. Katsanis, E. Matijević, *Colloids Surf.* **1982**, *5*, 43.
4 R. B. Wilhelmy, R. C. Patel, E. Matijević, *Inorg. Chem.* **1985**, *24*, 3290.
5 T. Ishikawa, E. Matijević, *J. Colloid Interface Sci.* **1988**, *123*, 122.
6 R. B. Wilhelmy, E. Matijević, *Colloids Surf.* **1987**, *22*, 97.
7 I. I. Springsteen, E. Matijević, *Colloid Polym. Sci.* **1989**, *267*, 1007.
8 K. Kandori, M. Toshioka, H. Nakashima, T. Ishikawa, *Langmuir* **1993**, *9*, 1031.
9 K. Kandori, H. Nakashima, T. Ishikawa, *J. Colloid Interface Sci.* **1993**, *160*, 499.
10 K. Kandori, T. Imazato, A. Yasukawa, T. Ishikawa, *Colloid Polym. Sci.* **1996**, *274*, 290.
11 K. Kandori, N. Ikeguchi, A. Yasukawa, T. Ishikawa, *J. Colloid Interface Sci.* **1996**, *182*, 425.
12 K. Kandori, N. Ikeguchi, A. Yasukawa, T. Ishikawa, *J. Colloid Interface Sci.* **1998**, *202*, 369.
13 K. Kandori, T. Kuwae, T. Ishikawa, *J. Colloid Interface Sci.* **2006**, *300*, 225.
14 T. Kawasaki, S. Takahashi, K. Ikeda, *Eur. J. Biochem.* **1985**, *152*, 361.
15 T. Kawasaki, M. Niikura, S. Takahashi, K. Kobayashi, *Biochem. Int.* **1986**, *13*, 969.
16 T. Kawasaki, K. Ikeda, S. Takahashi, Y. Kuboki, *Eur. J. Biochem.* **1986**, *155*, 249.
17 A. Tiselius, S. Hjertén, Ö. Levin, *Acrh. Biochem. Biophys.* **1956**, *65*, 132.
18 J. D. McGilvery, J. P. Crowther, *Can. J. Chem.* **1954**, *32*, 174.
19 R. P. Mitra, B. R. Thukral, *Indian J. Chem. Sect. A: Inorg., Bioinorg., Phys., Theor. Anal. Chem.* **1970**, *8*, 350.
20 Y. Miyazaki, G. Kura, H. Tsuzuki, H. Sakashita, *J. Chem. Soc., Faraday Trans.* **1996**, *92*, 3587.
21 R. K. Osterheld, in *Topics in Phosphorus Chemistry*, ed. by H. Barman, John Wiley & Sons Inc., **1972**, Vol. 7, p. 103.
22 J. G. Morales, R. R. Clemente, E. Matijević, *J. Colloid Interface Sci.* **1992**, *151*, 555.
23 F. Caruso, *Chem.—Eur. J.* **2000**, *6*, 413.
24 S. Schacht, O. Huo, I. G. Voigt-Martin, G. D. Stucky, F. Schüth, *Science* **1996**, *273*, 768.
25 Y. Ma, L. Qi, J. Ma, H. Cheng, *Langmuir* **2003**, *19*, 4040.
26 T. Liu, Y. Xie, B. Chu, *Langmuir* **2000**, *16*, 9015.
27 S.-H. Yu, H. Cölfen, M. Antonietti, *J. Phys. Chem. B* **2003**, *107*, 7396.
28 H. Cölfen, *Macromol. Rapid Commun.* **2001**, *22*, 219.
29 L. M. Qi, J. Li, J. Ma, *Adv. Mater.* **2002**, *14*, 300.
30 C. E. Fowler, M. Li, S. Mann, H. C. Margolis, *J. Mater. Chem.* **2005**, *15*, 3317.
31 T. Ohno, M. Aizawa, *Key Eng. Mater.* **2006**, *309–311*, 235.
32 H. T. Schmidt, M. Kroczynski, J. Maddox, Y. Chen, R. Josephs, A. E. Ostafin, *J. Microencapsulation* **2006**, *23*, 769.
33 W. Tjandra, P. Ravi, J. Yao, K. C. Tam, *Nanotechnology*

2006, *17*, 5988.
34 A. Bigi, E. Boanini, D. Walsh, S. Mann, *Angew. Chem., Int. Ed.* **2002**, *41*, 2163.
35 Q. Wang, W. Huang, D. Wang, B. W. Darvell, D. E. Day, M. N. Rahaman, *J. Mater. Sci.: Mater. Med.* **2006**, *17*, 641.
36 T. Sugimoto, S. Chen, A. Muramatsu, *Colloids Surf., A* **1998**, *135*, 207.
37 K. Kandori, S. Oda, S. Tsuyama, *J. Phys. Chem. B* **2008**, *112*, 2542.
38 K. S. W. Sing, D. H. Everett, R. A. W. Haul, L. Moscou, R. A. Pierotti, J. Rouquérol, T. Siemieniewska, *Pure Appl. Chem.* **1985**, *57*, 603.
39 F. S. Balker, K. S. W. Sing, L. J. Stryker, *Chem. Ind.* **1970**, *30*, 718.